

## Optical Properties of Single-Wall Carbon Nanotubes

H. Kataura<sup>a,\*</sup>, Y. Kumazawa<sup>a</sup>, Y. Maniwa<sup>a</sup>, I. Umezumi<sup>b</sup>, S. Suzuki<sup>c</sup>, Y. Ohtsuka<sup>c</sup> and Y. Achiba<sup>c</sup><sup>a</sup> Department of Physics, Faculty of Science, Tokyo Metropolitan University, 1-1 Minami-Ohsawa, Hachioji, Tokyo 192-0397, Japan<sup>b</sup> Department of Applied Physics, Faculty of Science, Konan University, 8-9-1 Okamoto Higashinadaku, Kobe 658-8501, Japan<sup>c</sup> Department of Chemistry, Faculty of Science, Tokyo Metropolitan University, 1-1 Minami-Ohsawa, Hachioji, Tokyo 192-0397, Japan**Abstract**

Four kinds of single-wall carbon nanotubes (SWNTs) with different diameter distribution have been synthesized and optical absorption spectra have been measured. Three large absorption bands due to the optical transitions between spike-like density of states, characteristics of SWNTs, were observed from infrared to visible region. Comparing with the calculated energy band, it has been concluded that the first and the second lowest absorption bands are due to the optical transitions between spikes in semiconductor phases and the third one is due to that in metallic phases. Absorption Peaks sensitively shifted to higher energy side with decreasing tube diameters as the band calculation predicted. Resonance Raman spectra were also measured using various laser lines. When the excitation is in an energy region corresponding to the absorption band of metallic phase, spectra have shown Breit-Wigner-Fano line shape, which is a sign of metallic phase. Using these results, we can easily characterize SWNTs from the optical absorption spectra without Raman measurements and transmission electron microscope observations.

*Keywords:* Infrared and Raman spectroscopy, UV-Vis-NIR absorption, Photothermal deflection spectroscopy, Graphite and related compounds

**1. Introduction**

From the discovery of the single-wall carbon nanotube (SWNT) by Iijima and Ichihashi [1], many investigators have studied this new form of carbon to clarify its attractive physical properties aiming for a development of future applications. [2] Theoretical works indicated that SWNT has characteristic electronic structure due to a low dimensionality, such as spike like density of states due to one-dimensional van Hove singularity. [3,4] Within a zone-folding scheme, one third of all the SWNTs are metallic and always have wider first energy gaps between spikes than semiconducting ones with almost the same diameters. Indeed, very recently, Wildöer *et al.* have directly observed electronic density of states of individual SWNTs by scanning tunneling spectroscopy and have shown a good agreement with the tight-binding zone-folding calculation. [5] On the other hand, Rao *et al.* have shown resonance Raman spectra of SWNTs for a wide energy region. [6] Very sharp resonant feature shows that optical transitions between spikes of density of states seem to enhance the Raman intensity. Thus, it is very interesting to measure optical absorption spectra of the SWNTs. Optical transition between spikes will be observed and different energy gap values in metallic and semiconducting SWNTs will be seen.

Technologies to synthesize SWNTs have greatly advanced to date. Both a double laser vaporization method using Ni/Co catalyst [7] and an electric arc method using Ni/Y catalyst [8] can synthesize very high concentration of SWNTs in a soot product.

Diameter control technique has also been advanced. For example, very thin SWNTs could be synthesized by laser vaporization of Rh/Pd catalyzed graphite rod. [9]

In this report, the optical absorption spectra of SWNTs with various diameter distributions will be shown. For an assignment of the spectra,  $\pi$  band of SWNT was calculated by tight-binding zone-folding method. Further, resonant Raman spectra for a wide excitation energy region will be shown.

**2. Experimental**

SWNTs were prepared by both laser vaporization and electric arc methods. Details of procedure of the laser vaporization method have been published previously, [10] and the electric arc method is quite conventional one. In the laser vaporization method, the second harmonic Nd:YAG laser pulse is focused on the metal catalyzed carbon rod settled in a quartz tube which was heated to 1200 °C by electric furnace and was filled 500 Torr Ar gas. Laser-vaporized carbon and catalyst finally became soot containing SWNTs and nanoparticles of the catalysts. In this method, we can control a diameter distribution of SWNTs changing a temperature of the furnace. On the other hand, the electric arc method has a simple procedure. DC arc between catalyzed carbon anode and pure carbon cathode produced SWNTs in 500Torr He. We can also control diameters of SWNTs with changing the pressure of He gas. Used catalysts for formation of SWNTs are NiY (4.2-1 at.%), NiCo (1.2 at.%), Ni

\*E-mail address: kataura@phys.metro-u.ac.jp.

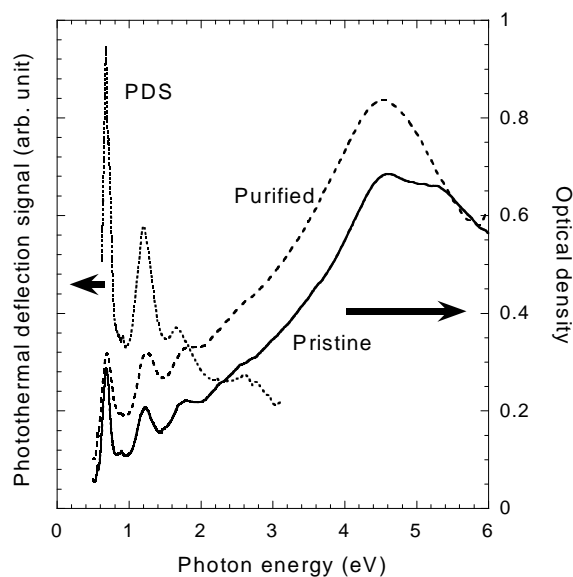


Fig. 1. Optical absorption spectra of SWNTs. Solid curve shows optical density of SWNTs film on quartz plate fabricated by electric arc method using NiY catalyst. Broken curve and Dotted curve show optical density and PDS signal of purified SWNTs (NiY), respectively. Due to the saturation of the PDS signal, intensity decreased with increasing photon energy and measurements were restricted up to 3 eV.

(0.6 at.%) and RhPd (1.2 at.%), which have provided another diameter distributions. In the case of NiY, web like SWNTs obtained by electric arc could be easily purified by heating in air at 350 °C for 30 minutes and by rinsing out metal particles in hydrochloric acid. Details will be described elsewhere.

Resonant Raman scattering was measured using 1 m double monochromator, JOBIN YVON U-1000, and photo-multiplier, HAMAMATSU PHOTONICS R943-02, with various laser systems, Ar laser, Nd:YAG laser, dye laser and Ti-sapphire laser. Since each laser has a different beam profile and a total sensitivity of measuring system changes with excitation wavelength, it is quite difficult to calibrate the relative intensity. To minimize these effects, in this paper, obtained Raman intensities were normalized by integrated Raman intensity of a crystalline Si that was also used as a standard of Raman shift.

A thin film of SWNTs was prepared by a painting method. The soot containing SWNTs was dispersed in ethanol homogeneously by supersonic waves, and was sprayed on a quartz plate using an airbrush with a hot air blow. The thickness and uniformity of the film were controlled by eyes. Optical transmittance spectra were measured with HITACHI U-3500 spectrophotometer.

The optical absorption spectrum was measured also by photothermal deflection spectroscopy (PDS) [11] for thermally purified SWNTs fabricated by the electric arc method using the NiY catalyst. This technique measures heat which is produced during relaxation of the electron hole pair generated by the absorbed light. The PDS has advantages to measure scattering materials since it measures optical absorption directly. In this measurement, carbon black was used as a black body reference. Thus the spectrum reflects the difference in electronic states between SWNTs and amorphous carbon.

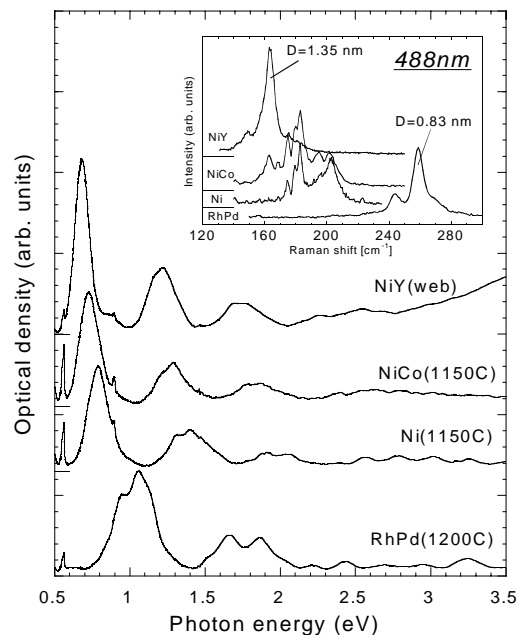


Fig. 2. Optical absorption spectra of four kinds of SWNTs with different diameter distributions. Background absorption due to the  $\pi$  plasmon was subtracted. Inset shows Raman spectra of the breathing mode, which provide a rough estimation of the diameter distribution. Electric arc method was used for NiY catalyst and all the other samples were synthesized by laser ablation method. Peaks at 0.55 and 0.9 eV are absorption by the quartz substrate.

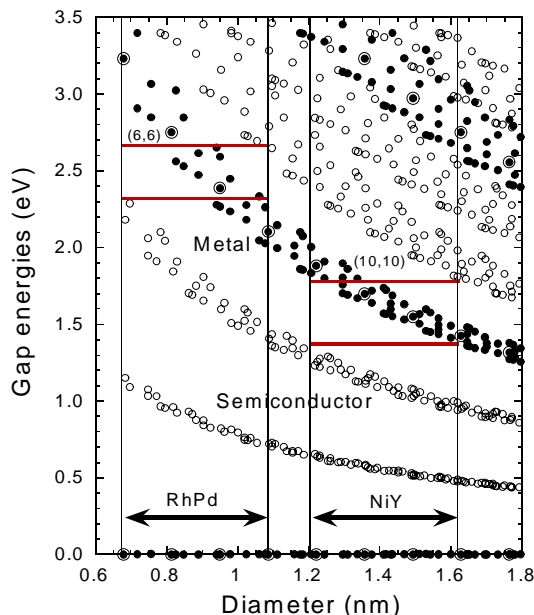


Fig. 3. Calculated gap energies between mirror-image spikes in density of states for  $\gamma = 2.75$  eV. Solid circles indicate the metallic SWNTs and open circles the semiconducting ones. Double circles indicate the armchair-type SWNTs. Gap energies for all the chiral indexes with larger diameter than (5,5) are plotted as a function of diameter. Arrows show diameter distributions for each catalyst. Two horizontal lines in each catalyst area show “metallic window” in which the optical transitions only by the metallic tubes would be observed.

### 3. Results and Discussion

From the transmission electron microscope (TEM) observation and  $A_{1g}$  breathing mode frequencies in Raman spectra, [12] it was found that diameters of SWNTs were distributed from 1.24 to 1.58 nm for NiY catalyst, from 1.06 to 1.45 nm for NiCo and Ni, and from 0.68 to 1.00 nm for RhPd. Most of the catalysts, except for the RhPd, show very similar diameter distribution for both the laser vaporization and the electric arc methods at a condition giving the highest yield. In the case of RhPd catalyst, however, none of SWNTs are synthesized by arc discharge in contrast with a high yield by laser vaporization method.

Solid curve in Fig. 1 shows optical absorption spectrum of SWNTs synthesized by the electric arc method using NiY catalyst. Three large absorption peaks at 0.68, 1.2 and 1.7 eV are superposed on the broad absorption due to  $\pi$  plasmon. To confirm that these peak structures are characteristics of SWNTs, it needs to be checked that the peaks are due to neither the absorption of metal catalysts remaining in the sample nor the light scattering losses by the soot. In the beginning, to remove the soot and catalyst, purification was performed as mentioned above and the decrease of nanosphere and catalysts was confirmed by TEM images and X-ray diffraction. Broken curve in Fig. 1 shows the absorption spectrum of the purified sample. Almost the same absorption structure with pristine sample indicates that the absorption structure is originated from SWNTs. As a second approach, optical absorption spectrum was measured by PDS, which is not affected by the light scattering. PDS signal is plotted in Fig. 1 with a dotted curve. Since carbon black powder was used as a reference, PDS signal reflects the difference in electronic states between amorphous carbon and SWNTs. Sharp absorption peaks are apparently observed almost the same position to the optical density, which indicates that these peaks are not due to the light scattering losses. Since it was recognized that the remaining nanosphere and metal particles do not affect the optical absorption spectrum, optical absorption spectra of pristine samples were adopted as those of the SWNTs.

Figure 2 shows the optical absorption spectra of SWNTs with different diameter distributions. For a convenience, large background due to  $\pi$  plasmon was subtracted. Inset shows the low frequency Raman spectra of the SWNTs. Diameter distributions can be estimated from the peak frequencies with a rule,  $\omega \propto 1/D$ , where  $D$  is a diameter of SWNT. [4] Thus, higher lying Raman peak indicates existence of smaller diameter of SWNT.

For all the samples, very similar absorption structures are seen. In the case of NiY catalyst, a sharp absorption band at 0.68 eV, slightly broad band at 1.2 eV and rather broad band at 1.7 eV are observed. This structure is kept in the case of NiCo and Ni catalysts but peak positions are considerably different. For example, in NiCo case, the first peak lies at 0.72 eV and in case of Ni catalyst, lies at 0.8 eV. In the thinnest case of RhPd, the first peak is observed around 1 eV and has shoulder. Further, the third absorption band is not observed clearly.

To explain these absorption spectra, band structure of SWNT was calculated using zone-folding method. [4] Tight-binding  $\pi$  band structure of two-dimensional graphite sheet is expressed by

$$E_{2D} = \pm \gamma \left\{ 1 + 4 \cos \left( \frac{\sqrt{3}k_x a}{2} \right) \cos \left( \frac{k_y}{2} \right) + 4 \cos^2 \left( \frac{k_y}{2} \right) \right\}^{1/2}. \quad (1)$$

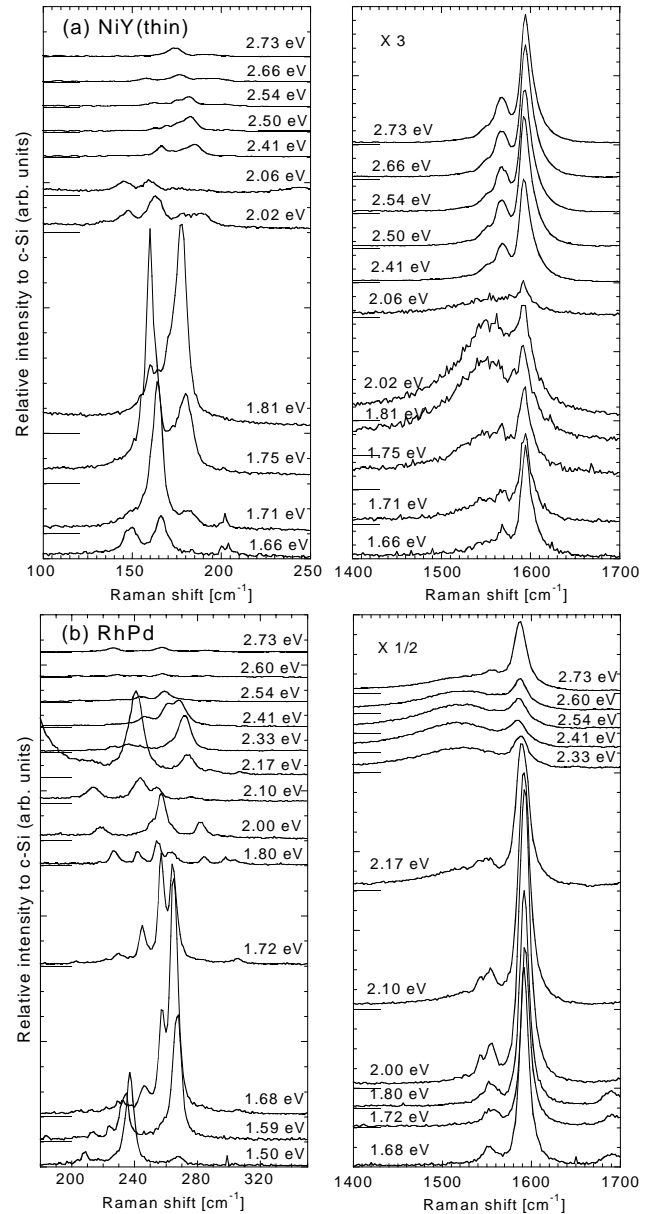


Fig. 4. Resonance Raman spectra of SWNTs. (a) SWNTs synthesized using NiY catalyst and (b) SWNTs using RhPd. For the discussion, SWNTs displayed in (a) have been chosen to have thinner diameter distribution than that in Fig. 2.

Here,  $\gamma$  is the overlap integral and  $a$  is a lattice constant. Using eq. (1), one-dimensional energy band of SWNT could be calculated applying a periodic boundary condition for any chiral vectors. Wave vector conserving optical transition would occur between mirror image spikes of density of states due to the one-dimensional van Hove singularities. Gap energies between the mirror spikes are indicated in Fig. 3. When the chiral index is expressed in  $(n_1, n_2)$ , the condition to be metallic is  $2n_1 + n_2 = 3l$ , where  $l$  is an integer. [4] Thus, one third of all the indexes show metallic character, which is indicated by circles on zero line and the other indexes are semiconducting, finite value of energy gaps. In Fig. 3, it is clear that the first and second lowest energy gaps between spikes come from the semiconducting tubes and the third

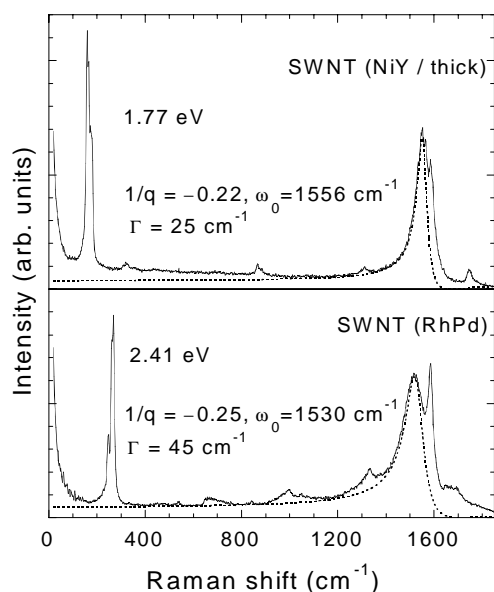


Fig. 5. Raman spectra of metallic SWNTs. Dotted curves show Breit-Wigner-Fano line shapes.

one comes from the metallic tubes with almost the same diameter. If the sample contain both type of SWNTs with indicated diameter distribution, SWNTs by NiY catalyst will show optical absorption peaks at 0.55, 1.1 and 1.7 eV and higher lying peak will have larger half width. On the other hand, in the case of RhPd, absorption peaks around 0.9 and 1.8 eV are expected but the third group by metallic tubes is extended too widely to be observed as an absorption band. These theoretical predictions show very good correspondences with experimental results shown in Fig. 2. Each absorption peak consists of a lot of narrow absorption peaks of constituent SWNTs. Indeed, observed each absorption peak in Fig. 2 has fine structures. From these analyses, we have concluded that the first and second absorption peaks are due to the semiconducting SWNTs and third one is due to the metallic SWNTs. If this is true, only metallic SWNTs will be resonated in Raman spectrum when the laser excitation is tuned at “metallic window” shown in Fig. 3.

Figure 4 (a) and 4(b) show the wide range resonance Raman spectra of SWNTs using NiY and RhPd catalysts, respectively. Relative Raman intensity of low frequency region is roughly proportional to the magnitude of optical absorption of SWNTs. At the high frequency region, broad and asymmetric Raman peak was observed around 1.8 eV for NiY case and around 2.4 eV for RhPd case, which correspond to the “metallic window”. This asymmetric Breit-Wigner-Fano (BWF) line shape was already reported by Rao *et al.* in K and Rb doped SWNTs. [13] The BWF line shape is given by

$$I(\omega) = I_0 \{1 + (\omega - \omega_0) / q\Gamma\}^2 / \{1 + ((\omega - \omega_0) / \Gamma)^2\}, \quad (2)$$

where  $I_0$ ,  $\omega_0$ ,  $\Gamma$  and  $q$  are intensity, renormalized frequency, broadening parameter and the lineshape parameter, respectively. Because of the broad resonance feature of high frequency Raman mode [14], there remain the sharp peaks from semiconducting SWNTs. Nevertheless, main part of Raman spectra in Fig.5 could be fitted with eq. (2) successfully. Fitting parameters are indicated in Fig. 5. This means that SWNTs on resonance are metallic,

while electronic scattering backgrounds are very small in both the spectra compared with the alkali metal doped systems. [13]

Now we return to the resonance Raman spectra in Fig. 4(a). At the “metallic window” region, from 1.66 to 1.81 eV, low frequency spectra show very simple feature. Only four large and rather broad peaks arise in this energy region. From their frequencies and resonance energies, these peaks are assigned as (16,4) for 154  $\text{cm}^{-1}$ , (10,10) for 163  $\text{cm}^{-1}$ , (18,0) for 157  $\text{cm}^{-1}$  and (12,6) for 178  $\text{cm}^{-1}$ . Since these SWNTs with even-even numbered indexes have small unit cells, they would show the strong Raman intensities. [12]

#### 4. Conclusion

Optical absorption spectra of SWNTs were measured and three large absorption peaks were observed. One-dimensional band calculation and resonance Raman scattering indicate that the first and second lowest peaks are due to optical transition between mirror image spikes in density of states of semiconducting tubes and the third one is due to metallic tubes. Since the peak position is very sensitive to the diameter like a breathing mode in the Raman spectrum, diameter distribution of the SWNTs can also be estimated from the absorption spectrum. Furthermore, the mixture ratio between the metallic and semiconducting tubes may roughly be estimated from the intensity ratio between absorption peaks due to metallic and semiconducting phases.

Ando [15] has shown that the considerable amount of the optical intensity is transferred to exciton bound states because of quasi one-dimensional nature of SWNTs. Indeed, the first absorption peak position is slightly higher than the calculated energy gap and corresponds to the exciton states under the Coulomb interaction.

#### Acknowledgements

The authors thank Prof. R. Saito for fruitful discussion about phonon mode in SWNT. The authors thank Mr. Misaki for TEM observations. This work was partially supported by Japan Society for the Promotion of Science Research for the Future Program and was partially supported by Grant-Aid for Scientific Research from Ministry of Education, Science and Culture.

#### References

- [1] S.Iijima and T. Ichihashi, *Nature* **363** (1993) 603.
- [2] P. G. Collins *et al.*, *Science* **278** (1997) 100.
- [3] N. Hamada *et al.*, *Phys. Rev. Lett.* **68** (1992) 1579.
- [4] R.Saito *et al.*, *Appl. Phys. Lett.* **60** (1992) 2204.
- [5] J.W.G. Wildöer *et al.*, *Nature* **391** (1998) 59.
- [6] A.M.Rao *et al.*, *Science* **275** (1997) 187.
- [7] A.Thess *et al.*, *Science* **273** (1996) 483.
- [8] C.Journet *et al.*, *Nature* **388** (1997) 756.
- [9] H.Kataura *et al.*, *Jpn. J. Appl. Phys.* **37** (1998) L616.
- [10] T.Wakabayashi *et al.*, *Z. Phys. D* **40** (1997) 414.
- [11] I.Umezu *et al.* *Jpn. J. Appl. Phys.* **33** (1994) L873.
- [12] R.Saito *et al.*, *Phys. Rev. B* **57** (1998) 4145.
- [13] A.M. Rao *et al.*, *Nature* **388** (1997) 257.
- [14] E. Richter and K.R.Subbaswamy, *Phys. Rev. Lett.* **79** (1997) 2738
- [15] T. Ando, *J. Phys. Soc. Jpn.* **66** (1997) 1066